

1 **Human basigin (CD147) does not directly interact with SARS-CoV-2 spike glycoprotein**

2 Robert J. Ragotte^{1,2}, David Pulido^{1,2}, Francesca R. Donnellan², Giacomo Gorini², Hannah
3 Davies², Juliane Brun³, Lloyd D. W. King², Katherine Skinner², Simon J. Draper^{2,4}.

4

5 ¹These authors contributed equally.

6 ²Jenner Institute, University of Oxford, Oxford, OX3 7DQ, UK.

7 ³Oxford Glycobiology Institute, Department of Biochemistry, University of Oxford, Oxford,
8 OX1 3RQ, UK

9 ⁴Corresponding author. Email: simon.draper@ndm.ox.ac.uk

10

11

12 **Abstract**

13 Basigin, or CD147, has been reported as a co-receptor used by SARS-CoV-2 to invade host
14 cells. Basigin also has a well-established role in *Plasmodium falciparum* malaria infection of
15 human erythrocytes where it is bound by one of the parasite's invasion ligands, reticulocyte
16 binding protein homolog 5 (RH5). Here, we sought to validate the claim that the receptor
17 binding domain (RBD) of SARS-CoV-2 spike glycoprotein can form a complex with basigin,
18 using RH5-basigin as a positive control. Using recombinantly expressed proteins, size
19 exclusion chromatography and surface plasmon resonance, we show that neither RBD nor
20 full-length spike glycoprotein bind to recombinant human basigin (either expressed in *E. coli*
21 or mammalian cells). Given the immense interest in SARS-CoV-2 therapeutic targets, we
22 would caution the inclusion of basigin in this list on the basis of its reported direct interaction
23 with SARS-CoV-2 spike glycoprotein.

24

25 **Importance**

26 Reducing the mortality and morbidity associated with COVID-19 remains a global
27 health priority. Critical to these efforts is the identification of host factors that are essential
28 to viral entry and replication. Basigin, or CD147, was previously identified as a possible
29 therapeutic target based on the observation that it may act as a co-receptor for SARS-CoV-2,
30 binding to the receptor binding domain of the spike protein. Here, we show that there is no
31 direct interaction between the RBD and basigin, casting doubt on its role as a co-receptor and
32 plausibility as a therapeutic target.

33

34 **Introduction**

35 Since the emergence of SARS-CoV-2 as the cause of the ongoing COVID-19 pandemic,
36 there has been a rush to identify therapeutic targets that could reduce the immense human
37 and economic toll of COVID-19. Receptors required for viral entry are a natural consideration
38 for druggable targets, as receptor-blockade could both prevent infection, if a drug is delivered
39 prophylactically, or treat infection in a therapeutic setting by stopping the spread of the virus
40 to other tissues and organs. Moreover, there may be existing monoclonal antibodies (mAbs)
41 approved for clinical use that target these receptors.

42 After the release of the genome sequence of SARS-CoV-2, the primary entry receptor
43 was rapidly identified as angiotensin converting enzyme 2 (ACE2) (1–5). This is the same entry
44 receptor used by some other coronaviruses, most notably SARS-CoV-1, a highly similar
45 coronavirus that emerged in 2002 (1, 6). Since this initial identification of ACE2, there has
46 been significant discussion in the literature, both peer-reviewed and pre-print, about other
47 co-receptors or co-factors required for entry (5, 7–9). Transmembrane protease, serine 2

48 (TMPRSS2) is one such co-factor that has been identified and subsequently validated by
49 multiple groups, which cleaves the spike protein to facilitate entry (5, 10, 11).

50 Another co-receptor that gained some attention is CD147, or basigin, which was first
51 described as a spike glycoprotein co-receptor in the pre-print literature in March 2020 and
52 which has since been published in a peer-reviewed journal (9). The authors suggest that spike
53 binding to basigin has important functional implications for viral entry, making basigin-
54 blockade an attractive therapeutic target (9). Since this initial finding, basigin has been
55 included in discussions of SARS-CoV-2 co-receptors (7, 12–20).

56 Basigin is ubiquitously expressed in human tissues, and forms a complex with
57 monocarboxylate transporters (MCTs), the glucose transporter GLUT1, integrins $\alpha_3\beta_1$ and
58 $\alpha_3\beta_1$, among others (21). In the context of infectious disease, basigin has also been well-
59 characterised as an essential receptor for *Plasmodium falciparum* invasion into human
60 erythrocytes, during which it is bound by the malaria parasite's reticulocyte binding protein
61 homolog 5 (RH5) (22, 23). Based on the initial observation that appeared to show basigin
62 binds to the SARS-CoV-2 spike glycoprotein receptor binding domain (RBD) (9), clinical trials
63 were initiated investigating an anti-basigin mAb as a therapeutic for COVID-19 (24)
64 (ClinicalTrials.gov identifier NCT04275245).

65 Having worked extensively with basigin in the context of its RH5 interaction, we aimed
66 to validate the finding that basigin directly interacts with the receptor binding domain of the
67 SARS-CoV-2 spike protein. Here, we show that we could not replicate this finding. Although
68 we see clear binding of recombinant SARS-CoV-2 full-length spike trimer (FL-S) and RBD to
69 ACE2 and the anti-RBD mAb CR3022 (25), we do not see any binding to glycosylated or non-
70 glycosylated basigin through size exclusion chromatography (SEC) or surface plasmon

71 resonance (SPR). Meanwhile, recombinant RH5 shows clear binding to both glycosylated and
72 non-glycosylated basigin through the same methods.
73

74 **Materials and Methods**

75 *Recombinant protein expression and purification*

76 A construct for soluble trimeric spike (FL-S) glycoprotein of SARS-CoV-2 (NCBI
77 Reference Sequence: YP_009724390.1), encoding residues M1-P1213 with two sets of
78 mutations that stabilise the protein in a pre-fusion conformation (removal of a furin cleavage
79 site and the introduction of two proline residues: K986P, V987P), was expressed as described
80 previously (26). This construct includes the endogenous viral signal peptide at the N-terminus
81 (residues 1-14), while a C-terminal T4-foldon domain is incorporated to promote association
82 of monomers into trimers to reflect the native transmembrane viral protein. The RBD
83 construct utilised the native SARS-CoV-2 spike signal peptide (1-14) fused directly to residues
84 R319-F541 of the spike glycoprotein which encompasses the binding site for the human
85 receptor ACE2 (26). Both constructs include a C-terminal hexa-histidine (His6) tag for nickel-
86 based affinity purification. FL-S and RBD were transiently expressed in Expi293™ cells (Thermo
87 Fisher Scientific) and protein purified from culture supernatants by immobilised metal affinity
88 followed by gel filtration in Tris-buffered saline (TBS) pH 7.4 buffer.

89 Full-length SARS-CoV-2 Nucleoprotein (FL-NP, NCBI Reference Sequence:
90 YP_009724397.2, residues M1-A419) was transiently expressed in Expi293™ cells (Thermo
91 Fisher Scientific) intracellularly. The FL-NP construct included a C-tag peptide (EPEA) at the C-
92 terminus (27) for affinity chromatography purification using a C-tag affinity resin (Thermo
93 Fisher Scientific), eluting with 20 mM Tris-HCl, 2 M MgCl₂ pH 7.4. Affinity purification was
94 followed by size exclusion chromatography in TBS pH 7.4 buffer. Human ACE2 ectodomain
95 (NCBI Reference Sequence: NP_001358344.1, residues Q18-S740) was expressed in Expi293™
96 cells (Thermo Fisher Scientific) with a preceding murine IgG1 signal peptide, monoFc domain
97 and TEV cleavage site at the N-terminus, and a GTGGG flexible linker and C-tag peptide at the

98 C-terminus. ACE2 containing supernatant was purified by C-tag affinity followed by size
99 exclusion chromatography in TBS pH 7.4 buffer. Human IgG1 CR3022 antibody (28) (GenBank:
100 ABA54613.1 and ABA54614.1) was expressed from heavy and light chain AbVec expression
101 vectors in Expi293™ cells (Thermo Fisher Scientific). CR3022 supernatant was purified using
102 HiTrap Protein G HP (Cytiva) followed by size exclusion chromatography in TBS pH 7.4 buffer.
103 Wild type/native human basigin (BSG-2, residues M1-L206) was expressed in Expi293™ cells
104 (Thermo Fisher Scientific) with C-terminal rat CD4 domains 3+4 (CD4d3+4) tag (to aid
105 expression and solubility) followed by a His6 tag for purification, as described previously (23,
106 29). Non-glycosylated basigin (also BSG-2) was expressed in *Escherichia coli* with an N-terminal
107 His6 tag followed by a TEV cleavage site, as described previously (22). The recombinant PfRH5
108 sequence is based on the *P. falciparum* 3D7 clone reference sequence and encodes amino
109 acids E26-Q526. The construct includes a C-terminal C-tag and four mutations to delete N-
110 linked glycosylation sequons (T40A, T216A, T286A and T299A). This construct was expressed
111 as a secreted protein by a stable *Drosophila* S2 cell line (30) and affinity purified using C-tag
112 affinity resin (Thermo Fisher Scientific) followed by a size-exclusion chromatography polishing
113 step in 20 mM Tris, 150 mM NaCl, pH 7.4.

114

115 *SEC binding assay*

116 100 µg of recombinant receptor (either mammalian-/*E. coli*-expressed basigin, or
117 ACE2) were mixed in a 1:1 molar ratio with RH5, FL-S, or RBD and then incubated for 1 h at
118 room temperature (RT). After incubation, samples were loaded onto a S200 10/300 column
119 via direct injection using an Äkta Pure (GE Healthcare) and run at 0.8 mL/min at RT. Eluted
120 fractions were collected and run on SDS-PAGE under reducing or non-reducing conditions
121 before staining with Coomassie blue.

122

123 *Protein Blots*

124 Samples were diluted 1:4 in Laemelli buffer, with or without dithiothreitol (DTT), and
125 then heated at 95 °C for 5 min before loading onto a pre-cast 4-12 % Bis-Tris polyacrylamide
126 gel (Thermo Fisher Scientific). Samples were run at 200 V for 45 min before staining with
127 Coomassie Blue.

128 1 µg FL-S or RBD were pipetted onto a 0.2 µm nitrocellulose membrane and allowed
129 to air dry. Immunoblotting was performed using the Invitrogen iBind Western System
130 according to manufacturer's instructions. CR3022 was used as a primary antibody diluted to
131 2 µg/mL. Alkaline phosphatase conjugated goat anti-human IgG, Fc-specific, (Sigma) diluted
132 to 1:2000 was used for detection with Sigmafast BCIP/NBT alkaline phosphatase substrate at
133 1 mg/mL (Sigma-Aldrich).

134

135 *Surface plasmon resonance*

136 Basigin, either mammalian- or *E. coli*-expressed, was immobilised on a CM5 chip
137 through amine conjugation using NHS/EDC coupling using a Biacore X100 (GE Healthcare).
138 Samples were run at 30 µL/min with an injection time of 60 s and a dissociation of 200 s. Then
139 5-step two-fold dilution curves of either RH5, RBD or FL-NP were run over starting at 2 µM,
140 with regeneration of the chip via injection of 10 mM glycine pH 2 for 30 s. Between runs, a
141 single injection of RH5 at 2 µM was carried out to confirm there was no loss in binding activity.
142 For CR3022 binding affinity, approximately 400 response units (RU) of antibody were
143 captured on a protein A chip. Steady-state affinity was determined through an 8-step dilution
144 curve beginning at 1 µM, with 10 mM glycine pH 2 used to regenerate the chip between

145 curves. All curves included one duplicate concentration and were evaluated using the Biacore
146 X100 evaluation software.

147

148 *PNGase F treatment*

149 PNGase F treatment was conducted as per manufacturer's protocol (New England
150 Biolabs). Briefly, 10 μ L of basigin at 0.5 μ g/ μ L expressed in either *E. coli* or Expi293TM cells
151 underwent denaturation at 95 $^{\circ}$ C for 10 min in glycoprotein denaturing buffer (New England
152 Biolabs) followed by immediate cooling on ice for 10 s. Then, the denatured protein was
153 mixed with 2 μ L of GlycoBuffer 2, 2 μ L 10 % NP-40, 6 μ L of water and 1 μ L of PNGase F. After
154 incubation for 1 h at 37 $^{\circ}$ C, samples were analysed by non-reducing SDS-PAGE and stained
155 with Coomassie Blue.

156 **Results**

157 *Spike and RBD bind human ACE2 via SEC*

158 Initially we produced a panel of recombinant protein reagents. Recombinant human
159 ACE2, SARS-CoV-2 full length spike trimer (FL-S), full-length nucleoprotein (FL-NP), Spike RBD
160 and anti-RBD antibody CR3022 were all expressed by transient transfection in mammalian
161 Expi293™ cells (**Fig. 1A,B**). Glycosylated and non-glycosylated basigin were expressed in
162 Expi293™ and *E. coli* respectively and glycosylation states confirmed by PNGaseF digest (**Fig.**
163 **S1**). Correct folding of RBD and FL-S was confirmed via dot blot using CR3022, a known SARS-
164 CoV-2 RBD and FL-S binding mAb (28), as the primary antibody (**Fig. 1C**). These data showed
165 all proteins expressed as expected and demonstrated high levels of purity. The FL-S and RBD
166 also showed stability upon freeze-thawing, and retained binding of the conformation-
167 sensitive mAb CR3022 after three freeze-thaw cycles (**Fig. 1C**).

168 We next confirmed SARS-CoV-2 RBD and FL-S binding to human ACE2 using SEC (**Fig.**
169 **2A**). When both RBD and ACE2 were incubated together, the complex eluted at an earlier
170 retention volume as compared to ACE2 alone, indicative of the formation of a higher
171 molecular weight complex. Complex formation was then confirmed using SDS-PAGE whereby
172 both RBD and ACE2 eluted within the same peak at approximately 10 mL, whereas RBD alone
173 normally elutes at approximately 16 mL (**Fig. 2A**).

174 This was next confirmed in the same manner with FL-S trimer, which also eluted as a
175 complex with ACE2 when incubated together, as shown by SDS-PAGE (**Fig. 2B**). Although there
176 is only a small change in retention volume between FL-S alone and the FL-S-ACE2 complex,
177 this can be attributed to the use of an S200 column, whose resolution limits are less than the
178 expected size of the FL-S-ACE2 complex (approximately 680 kDa). Nonetheless, it is clear that
179 the ACE2 eluted with FL-S at approximately 8 mL retention volume, whilst ACE2 alone eluted

180 at approximately 11 mL (**Fig. 2B**). We next demonstrated there was no interaction between
181 the RH5 malaria antigen and ACE2 (as expected), given both proteins eluted at the same
182 retention volume whether alone or mixed together (**Fig. 2C**). These results confirm that our
183 recombinant FL-S, RBD and ACE2 demonstrate the established interactions.

184

185 *SARS-CoV-2 spike and RBD do not bind human basigin via SEC*

186 Having confirmed the interaction between FL-S/RBD and ACE2, we proceeded to
187 assess FL-S and RBD binding to glycosylated human basigin using the same methodology. RH5,
188 which acted as the positive control, showed clear binding to basigin, forming a stable complex
189 in solution as confirmed by SEC and SDS-PAGE (**Fig. 2F**). Binding affinity between RH5 and
190 basigin is weaker than the reported values for RBD and basigin (approximately 1 μ M for RH5
191 (22, 23) compared to 185 nM for RBD (9)) indicating that this assay should be sufficiently
192 sensitive to detect the RBD-basigin interaction.

193 SARS-CoV-2 FL-NP was used as a negative control and did not form a complex with
194 basigin. Coincidentally, both FL-NP and basigin elute at the same retention volume, but the
195 absence of any shift to a higher order molecular weight complex when incubated together is
196 consistent with no complex formation (**Fig. 2G**). Next, we observed that there was no
197 detectable binding between either RBD or FL-S and glycosylated basigin, with both RBD and
198 FL-S eluting separately from basigin (**Fig. 2D,E**). Thus, it did not appear that any complex could
199 be formed in solution between these proteins.

200 Finally, in order to confirm whether glycosylation may affect binding, we performed
201 the experiment again using basigin ectodomain expressed in *E. coli* (**Fig. S1**), as described by
202 Wright *et al.* (22). Again, there was clear binding to RH5, but no discernible binding to either
203 of the FL-S or RBD proteins (**Fig. S2**).

204

205 *SARS-CoV-2 spike and RBD do not bind to human basigin via SPR*

206 Although it was clear the reported FL-S/RBD-basigin complex was not stable enough
207 to detect via SEC, we next sought to confirm the previously reported SPR data showing the
208 RBD-basigin interaction (9). To begin, we confirmed that the RBD protein interacted with
209 CR3022 with the expected affinity, via an 8-step dilution curve beginning at 1 μ M. The steady
210 state affinity was determined to be 190 nM, consistent with published data on this interaction
211 (25) (**Fig. 3A,B**).

212 Next basigin, either glycosylated (**Fig. 4A-C**) or non-glycosylated (**Fig. 4D-F**), was
213 immobilised through amine conjugation on a CM5 chip. RH5, RBD, or FL-NP were then flowed
214 over the chip to determine binding and affinity. RH5 clearly bound to both forms of basigin
215 with a steady-state affinity of approximately 925 ± 16 nM for bacterially-expressed basigin and
216 665 ± 39 nM for mammalian-expressed basigin, in line with previous reports (22, 23) (**Fig.**
217 **4A,D**). However, RBD did not show any discernible binding to either glycosylated (**Fig. 4B**) or
218 non-glycosylated basigin (**Fig. 4E**). FL-NP also did not bind to either form of basigin, as
219 expected (**Fig. 4C,F**).

220

221 **Discussion**

222 Here, we show that neither SARS-CoV-2 RBD nor full-length spike trimer bind to
223 recombinant human basigin. This is contrary to a previous report in the literature which
224 identified basigin as a co-receptor for SARS-CoV-2 and showed binding of RBD to spike via
225 SPR- and ELISA-based assays (9). The use of anti-basigin mAb in clinical trial has begun on the
226 basis of the original observation that basigin may be required for host cell entry (24). We
227 believe it is necessary to proceed with caution when interpreting the trial data, as further
228 investigation is warranted to determine what role, if any, basigin has in the SARS-CoV-2
229 invasion process.

230 Our findings here are also supported by another independent investigation (31). Shilts
231 *et al.* also show evidence that there is no direct interaction between CD147 and full-length
232 spike or its S1 domain using a different set of methods than used here (avidity-based
233 extracellular interaction screening and tetramer-staining of HEK293 cells expressing basigin)
234 (31). Their studies complement the work described here, as they also evaluated this
235 interaction using two different isoforms of basigin and in a cellular invasion assay (31),
236 whereas here we only evaluated the far more abundant basigin-2 isoform (32).

237 Initial evaluation of meplazumab, an anti-basigin antibody, for treatment of SARS-
238 CoV-2 pneumonia suggested there could be a benefit; however, we interpret these claims
239 with the utmost caution due to the lack of a peer reviewed publication at present and
240 exceedingly small group sizes (24). If indeed these findings hold, it could be due to non-
241 specific anti-inflammatory effect of basigin blockade, as there have been some reports of a
242 pro-inflammatory role of basigin in immune signalling (33–37). Alternatively, other viruses
243 have been reported to utilize CD147 to aid cellular invasion via indirect interactions –
244 including HIV-1 (38) and human cytomegalovirus (HCMV) (39), and these interactions can

245 show cell-type dependence. The *in vitro* effects of meplazumab on SARS-CoV-2 infection and
246 association of this process with endocytosis reported by Wang *et al.* could reflect a similar
247 phenomenon (9); although the basigin knock-down data reported by Shilts *et al.* in the lung
248 epithelial cell line (CaLu-3) would argue against this. Regardless, the benefit of meplazumab
249 is unlikely to be due to the direct inhibition of viral entry, due to the fact that SARS-CoV-2
250 spike protein does not appear to interact with basigin in our study or that of Shilts *et al.* (31)..

251 Nevertheless, the data surrounding the safety and tolerability of anti-basigin may have
252 implications beyond SARS-CoV-2, as these trials could inform the use of anti-basigin as a
253 malaria prophylactic regardless of its effectiveness in reducing mortality and morbidity due
254 to COVID-19. To date, this has not been pursued in the malaria field beyond *in vitro* assays
255 (40) or humanised mouse models (41), despite demonstration of remarkable potency of anti-
256 basigin mAbs. This is largely due to safety concerns regarding prophylactics that would target
257 a human host protein, as opposed to the parasite, in a vulnerable/infant target population.
258 Should this therapy prove to be safe and well-tolerated, it could be further explored in malaria
259 where basigin has a well-established role in pathogen invasion.

260

261 **Conclusion**

262 Recombinant basigin (CD147) does not bind directly to the SARS-CoV-2 RBD. The data
263 presented here do not support the role of basigin as a possible SARS-CoV-2 co-receptor.

264

265 **Acknowledgments**

266 The authors are grateful for the assistance of Julie Furze, Amy Boyd, Teresa Lambe (University
267 of Oxford); also to Alain Townsend (University of Oxford) for providing the ACE2 and CR3022
268 plasmids and Florian Krammer (Icahn School of Medicine at Mount Sinai) for providing the

269 spike and RBD plasmids. The development of SARS-CoV-2 reagents was partially supported
270 by the NIAID Centers of Excellence for Influenza Research and Surveillance (CEIRS) contract
271 HHSN272201400008C.

272

273 RJR is funded by the Wellcome Trust Infection, Immunology, and Translational Medicine D.
274 Phil programme, a Rhodes scholarship, and a Canadian Institutes of Health Research Doctoral
275 Foreign Study Award (FRN:157835). FRD holds a UK Medical Research Council (MRC) iCASE
276 PhD studentship (MR/N01796X/1). JB is supported by a Wellcome Trust PhD Programme
277 (203853/Z/16/Z). SJD is a Jenner Investigator, a Lister Institute Research Prize Fellow and a
278 Wellcome Trust Senior Fellow [106917/Z/15/Z]. For the purpose of Open Access, the authors
279 have applied a CC BY public copyright licence to any Author Accepted Manuscript version
280 arising from this submission.

281

282 **Author Contributions**

283 RJR, DP, and SJD conceived of the study. RJR, DP and SJD wrote the manuscript. RJR, DP, FRD,
284 GG, HD, JB and LDWK performed experiments. RJR, DP and SJD performed data analysis and
285 interpreted results. KS performed project management. RJR, DP, FRD, GG, HD, JB, LDWK, KS,
286 and SJD reviewed the final manuscript.

287

288 **Data and Materials Availability**

289 Requests for materials should be addressed to the corresponding author.

290

291 **Conflicts of Interest Statement**

292 SJD is a named inventor on patent applications relating to RH5 malaria vaccines and/or
293 antibodies.

294

295 **References**

296 1. Letko M, Marzi A, Munster V. 2020. Functional assessment of cell entry and receptor
297 usage for SARS-CoV-2 and other lineage B betacoronaviruses. *Nat Microbiol* 5:562–
298 569.

299 2. Shang J, Ye G, Shi K, Wan Y, Luo C, Aihara H, Geng Q, Auerbach A, Li F. 2020.
300 Structural basis of receptor recognition by SARS-CoV-2. *Nature* 581:221–224.

301 3. Yan R, Zhang Y, Li Y, Xia L, Guo Y, Zhou Q. 2020. Structural basis for the recognition of
302 SARS-CoV-2 by full-length human ACE2. *Science* 367:1444–1448.

303 4. Wang Q, Zhang Y, Wu L, Niu S, Song C, Zhang Z, Lu G, Qiao C, Hu Y, Yuen K-Y, Wang Q,
304 Zhou H, Yan J, Qi J. 2020. Structural and Functional Basis of SARS-CoV-2 Entry by
305 Using Human ACE2. *Cell* 181:894-904.e9.

306 5. Hoffmann M, Kleine-Weber H, Schroeder S, Krüger N, Herrler T, Erichsen S,
307 Schiergens TS, Herrler G, Wu N-H, Nitsche A, Müller MA, Drosten C, Pöhlmann S.
308 2020. SARS-CoV-2 Cell Entry Depends on ACE2 and TMPRSS2 and Is Blocked by a
309 Clinically Proven Protease Inhibitor. *Cell* 181:271-280.e8.

310 6. Li W, Moore MJ, Vasilieva N, Sui J, Wong SK, Berne MA, Somasundaran M, Sullivan JL,
311 Luzuriaga K, Greenough TC, Choe H, Farzan M. 2003. Angiotensin-converting enzyme
312 2 is a functional receptor for the SARS coronavirus. *Nature* 426:450–454.

313 7. Ng K, Faulkner N, Cornish G, Rosa A, Earl C, Wrobel A, Benton D, Roustan C, Bolland
314 W, Thompson R, Agua-Doce A, Hobson P, Heaney J, Rickman H, Paraskevopoulou S,
315 Houlihan CF, Thomson K, Sanchez E, Shin GY, Spyer MJ, Walker PA, Kjaer S, Riddell A,

- 316 Beale R, Swanton C, Gandhi S, Stockinger B, Gamblin S, McCoy LE, Cherepanov P,
317 Nastouli E, Kassiotis G. 2020. Pre-existing and humoral immunity to SARS-CoV-2 in
318 humans. *bioRxiv* 2020.05.14.095414.
- 319 8. Herrera NG, Morano NC, Celikgil A, Georgiev GI, Malonis RJ, Lee JH, Tong K, Vergnolle
320 O, Massimi AB, Yen LY, Noble AJ, Kopylov M, Bonanno JB, Garrett-Thomson SC, Hayes
321 DB, Bortz RH, Wirchnianski AS, Florez C, Laudermilch E, Haslwanter D, Fels JM,
322 Dieterle ME, Jangra RK, Barnhill J, Mengotto A, Kimmel D, Daily JP, Pirofski L,
323 Chandran K, Brenowitz M, Garforth SJ, Eng ET, Lai JR, Almo SC. 2020. Characterization
324 of the SARS-CoV-2 S Protein: Biophysical, Biochemical, Structural, and Antigenic
325 Analysis. *bioRxiv* 2020.06.14.150607.
- 326 9. Wang K, Chen W, Zhang Z, Deng Y, Lian J-Q, Du P, Wei D, Zhang Y, Sun X-X, Gong L,
327 Yang X, He L, Zhang L, Yang Z, Geng J-J, Chen R, Zhang H, Wang B, Zhu Y-M, Nan G,
328 Jiang J-L, Li L, Wu J, Lin P, Huang W, Xie L, Zheng Z-H, Zhang K, Miao J-L, Cui H-Y,
329 Huang M, Zhang J, Fu L, Yang X-M, Zhao Z, Sun S, Gu H, Wang Z, Wang C-F, Lu Y, Liu Y-
330 Y, Wang Q-Y, Bian H, Zhu P, Chen Z-N. 2020. CD147-spike protein is a novel route for
331 SARS-CoV-2 infection to host cells. *Signal Transduct Target Ther* 5:283.
- 332 10. Matsuyama S, Nao N, Shirato K, Kawase M, Saito S, Takayama I, Nagata N, Sekizuka T,
333 Katoh H, Kato F, Sakata M, Tahara M, Kutsuna S, Ohmagari N, Kuroda M, Suzuki T,
334 Kageyama T, Takeda M. 2020. Enhanced isolation of SARS-CoV-2 by TMPRSS2-
335 expressing cells. *Proc Natl Acad Sci* 117:7001–7003.
- 336 11. Zang R, Castro MFG, McCune BT, Zeng Q, Rothlauf PW, Sonnek NM, Liu Z, Brulois KF,
337 Wang X, Greenberg HB, Diamond MS, Ciorba MA, Whelan SPJ, Ding S. 2020. TMPRSS2
338 and TMPRSS4 promote SARS-CoV-2 infection of human small intestinal enterocytes.
339 *Sci Immunol* 5:eabc3582.

- 340 12. Radzikowska U, Ding M, Tan G, Zhakparov D, Peng Y, Wawrzyniak P, Wang M, Li S,
341 Morita H, Altunbulakli C, Reiger M, Neumann AU, Lunjani N, Traidl-Hoffmann C,
342 Nadeau K, O'Mahony L, Akdis CA, Sokolowska M. 2020. Distribution of ACE2, CD147,
343 CD26 and other SARS-CoV-2 associated molecules in tissues and immune cells in
344 health and in asthma, COPD, obesity, hypertension, and COVID-19 risk factors. *Allergy*
345 10.1111/all.14429.
- 346 13. Ulrich H, Pillat MM. 2020. CD147 as a Target for COVID-19 Treatment: Suggested
347 Effects of Azithromycin and Stem Cell Engagement. *Stem cell Rev reports* 16:434–440.
- 348 14. Zhou H, Fang Y, Xu T, Ni W-J, Shen A-Z, Meng X-M. 2020. Potential therapeutic targets
349 and promising drugs for combating SARS-CoV-2. *Br J Pharmacol* 177:3147–3161.
- 350 15. Ilikci Sagkan R, Akin-Bali DF. 2020. Structural variations and expression profiles of the
351 SARS-CoV-2 host invasion genes in lung cancer. *J Med Virol*
352 <https://doi.org/10.1002/jmv.26107>.
- 353 16. Ahmetaj-Shala B, Vaja R, Atanur SS, George PM, Kirkby NS, Mitchell JA. 2020.
354 Cardiorenal tissues express SARS-CoV-2 entry genes and basigin (BSG/CD147)
355 increases with age in endothelial cells. *JACC Basic to Transl Sci*
356 10.1016/j.jacbts.2020.09.010.
- 357 17. Matusiak M, Schürch CM. 2020. Expression of SARS-CoV-2 entry receptors in the
358 respiratory tract of healthy individuals, smokers and asthmatics. *Respir Res* 21:252.
- 359 18. Latini A, Agolini E, Novelli A, Borgiani P, Giannini R, Gravina P, Smarrazzo A, Dauri M,
360 Andreoni M, Rogliani P, Bernardini S, Helmer-Citterich M, Biancolella M, Novelli G.
361 2020. COVID-19 and Genetic Variants of Protein Involved in the SARS-CoV-2 Entry into
362 the Host Cells. *Genes (Basel)* 11:1010.
- 363 19. Singh M, Bansal V, Feschotte C. 2020. A Single-Cell RNA Expression Map of Human

- 364 Coronavirus Entry Factors. *Cell Rep* 32.
- 365 20. Zamorano Cuervo N, Grandvaux N. 2020. ACE2: Evidence of role as entry receptor for
366 SARS-CoV-2 and implications in comorbidities. *Elife* 9:e61390.
- 367 21. Muramatsu T. 2016. Basigin (CD147), a multifunctional transmembrane glycoprotein
368 with various binding partners. *J Biochem* 159:481–490.
- 369 22. Wright KE, Hjerrild KA, Bartlett J, Douglas AD, Jin J, Brown RE, Illingworth JJ, Ashfield
370 R, Clemmensen SB, de Jongh WA, Draper SJ, Higgins MK. 2014. Structure of malaria
371 invasion protein RH5 with erythrocyte basigin and blocking antibodies. *Nature*
372 515:427–430.
- 373 23. Crosnier C, Bustamante LY, Bartholdson SJ, Bei AK, Theron M, Uchikawa M, Mboup S,
374 Ndir O, Kwiatkowski DP, Duraisingh MT, Rayner JC, Wright GJ. 2011. Basigin is a
375 receptor essential for erythrocyte invasion by *Plasmodium falciparum*. *Nature*
376 480:534–537.
- 377 24. Bian H, Zheng Z-H, Wei D, Zhang Z, Kang W-Z, Hao C-Q, Dong K, Kang W, Xia J-L, Miao
378 J-L, Xie R-H, Wang B, Sun X-X, Yang X-M, Lin P, Geng J-J, Wang K, Cui H-Y, Zhang K,
379 Chen X-C, Tang H, Du H, Yao N, Liu S-S, Liu L-N, Zhang Z, Gao Z-W, Nan G, Wang Q-Y,
380 Lian J-Q, Chen Z-N, Zhu P. 2020. Meplazumab treats COVID-19 pneumonia: an open-
381 labelled, concurrent controlled add-on clinical trial. *medRxiv* 2020.03.21.20040691.
- 382 25. Yuan M, Wu NC, Zhu X, Lee C-CD, So RTY, Lv H, Mok CKP, Wilson IA. 2020. A highly
383 conserved cryptic epitope in the receptor binding domains of SARS-CoV-2 and SARS-
384 CoV. *Science* 368:630–633.
- 385 26. Amanat F, Stadlbauer D, Strohmeier S, Nguyen THO, Chromikova V, McMahon M,
386 Jiang K, Arunkumar GA, Jurczynszak D, Polanco J, Bermudez-Gonzalez M, Kleiner G,
387 Aydillo T, Miorin L, Fierer DS, Lugo LA, Kojic EM, Stoeber J, Liu STH, Cunningham-

- 388 Rundles C, Felgner PL, Moran T, García-Sastre A, Caplivski D, Cheng AC, Kedzierska K,
389 Vapalahti O, Hepojoki JM, Simon V, Krammer F. 2020. A serological assay to detect
390 SARS-CoV-2 seroconversion in humans. *Nat Med* 26:1033–1036.
- 391 27. Jin J, Hjerrild KA, Silk SE, Brown RE, Labbe GM, Marshall JM, Wright KE, Bezemer S,
392 Clemmensen SB, Biswas S, Li Y, El-Turabi A, Douglas AD, Hermans P, Detmers FJ, de
393 Jongh WA, Higgins MK, Ashfield R, Draper SJ. 2017. Accelerating the clinical
394 development of protein-based vaccines for malaria by efficient purification using a
395 four amino acid C-terminal “C-tag.” *Int J Parasitol* 47:435–446.
- 396 28. Wang C, Li W, Drabek D, Okba NMA, van Haperen R, Osterhaus ADME, van Kuppeveld
397 FJM, Haagmans BL, Grosveld F, Bosch B-J. 2020. A human monoclonal antibody
398 blocking SARS-CoV-2 infection. *Nat Commun* 11:2251.
- 399 29. Alanine DGW, Quinkert D, Kumarasingha R, Mehmood S, Donnellan FR, Minkah NK,
400 Dadonaite B, Diouf A, Galaway F, Silk SE, Jamwal A, Marshall JM, Miura K, Foquet L,
401 Elias SC, Labbé GM, Douglas AD, Jin J, Payne RO, Illingworth JJ, Pattinson DJ, Pulido D,
402 Williams BG, de Jongh WA, Wright GJ, Kappe SHI, Robinson C V, Long CA, Crabb BS,
403 Gilson PR, Higgins MK, Draper SJ. 2019. Human Antibodies that Slow Erythrocyte
404 Invasion Potentiate Malaria-Neutralizing Antibodies. *Cell* 178:216-228.e21.
- 405 30. Hjerrild KA, Jin J, Wright KE, Brown RE, Marshall JM, Labbé GM, Silk SE, Cherry CJ,
406 Clemmensen SB, Jørgensen T, Illingworth JJ, Alanine DGW, Milne KH, Ashfield R, de
407 Jongh WA, Douglas AD, Higgins MK, Draper SJ. 2016. Production of full-length soluble
408 Plasmodium falciparum RH5 protein vaccine using a Drosophila melanogaster
409 Schneider 2 stable cell line system. *Sci Rep* 6:30357.
- 410 31. Shilts J, Crozier TWM, Greenwood EJD, Lehner PJ, Wright GJ. 2021. No evidence for
411 basigin/CD147 as a direct SARS-CoV-2 spike binding receptor. *Sci Rep* 11:413.

- 412 32. Liao C-G, Kong L-M, Song F, Xing J-L, Wang L-X, Sun Z-J, Tang H, Yao H, Zhang Y, Wang
413 L, Wang Y, Yang X-M, Li Y, Chen Z-N. 2011. Characterization of basigin isoforms and
414 the inhibitory function of basigin-3 in human hepatocellular carcinoma proliferation
415 and invasion. *Mol Cell Biol* 31:2591–2604.
- 416 33. Peng C, Zhang S, Lei L, Zhang X, Jia X, Luo Z, Huang X, Kuang Y, Zeng W, Su J, Chen X.
417 2017. Epidermal CD147 expression plays a key role in IL-22-induced psoriatic
418 dermatitis. *Sci Rep* 7:44172.
- 419 34. Wang Q, Xu B, Fan K, Wu J, Wang T. 2020. Inflammation suppression by
420 dexamethasone via inhibition of CD147-mediated NF- κ B pathway in collagen-induced
421 arthritis rats. *Mol Cell Biochem* <https://doi.org/10.1007/s11010-020-03808-5>.
- 422 35. Jin R, Zhong W, Liu S, Li G. 2019. CD147 as a key mediator of the spleen inflammatory
423 response in mice after focal cerebral ischemia. *J Neuroinflammation* 16:198.
- 424 36. Supper V, Schiller HB, Paster W, Forster F, Boulègue C, Mitulovic G, Leksa V,
425 Ohradnova-Repic A, Machacek C, Schatzlmaier P, Zlabinger GJ, Stockinger H. 2016.
426 Association of CD147 and Calcium Exporter PMCA4 Uncouples IL-2 Expression from
427 Early TCR Signaling. *J Immunol* 196:1387–1399.
- 428 37. Dawar FU, Xiong Y, Khattak MNK, Li J, Lin L, Mei J. 2017. Potential role of cyclophilin A
429 in regulating cytokine secretion. *J Leukoc Biol* 102:989–992.
- 430 38. Pushkarsky T, Zybarth G, Dubrovsky L, Yurchenko V, Tang H, Guo H, Toole B, Sherry B,
431 Bukrinsky M. 2001. CD147 facilitates HIV-1 infection by interacting with virus-
432 associated cyclophilin A. *Proc Natl Acad Sci U S A* 98:6360–6365.
- 433 39. Vanarsdall AL, Pritchard SR, Wisner TW, Liu J, Jardetzky TS, Johnson DC. 2018. CD147
434 Promotes Entry of Pentamer-Expressing Human Cytomegalovirus into Epithelial and
435 Endothelial Cells. *MBio* 9:e00781-18.

- 436 40. Douglas AD, Williams AR, Knuepfer E, Illingworth JJ, Furze JM, Crosnier C, Choudhary
437 P, Bustamante LY, Zakutansky SE, Awuah DK, Alanine DG, Theron M, Worth A,
438 Shimkets R, Rayner JC, Holder AA, Wright GJ, Draper SJ. 2014. Neutralization of
439 Plasmodium falciparum merozoites by antibodies against PfRH5. *J Immunol* 192:245–
440 258.
- 441 41. Zenonos ZA, Dummler SK, Müller-Sienerth N, Chen J, Preiser PR, Rayner JC, Wright GJ.
442 2015. Basigin is a druggable target for host-oriented antimalarial interventions. *J Exp*
443 *Med* 212:1145–1151.
- 444

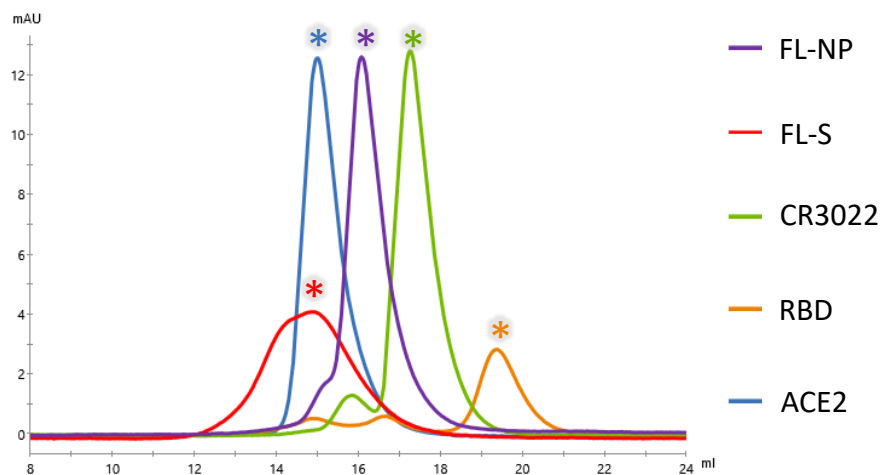
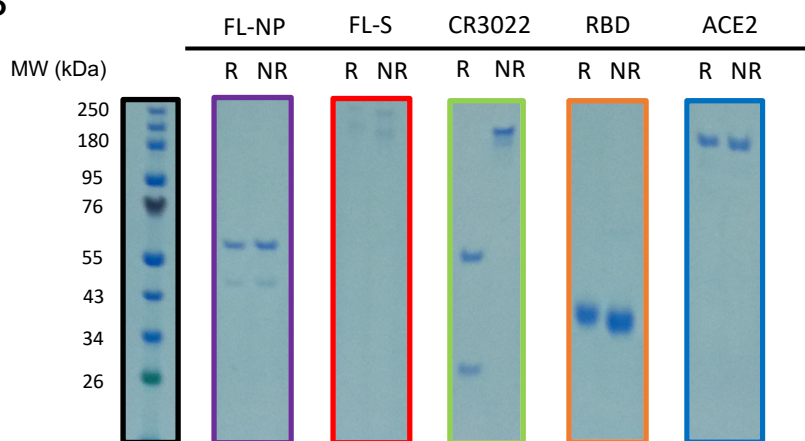
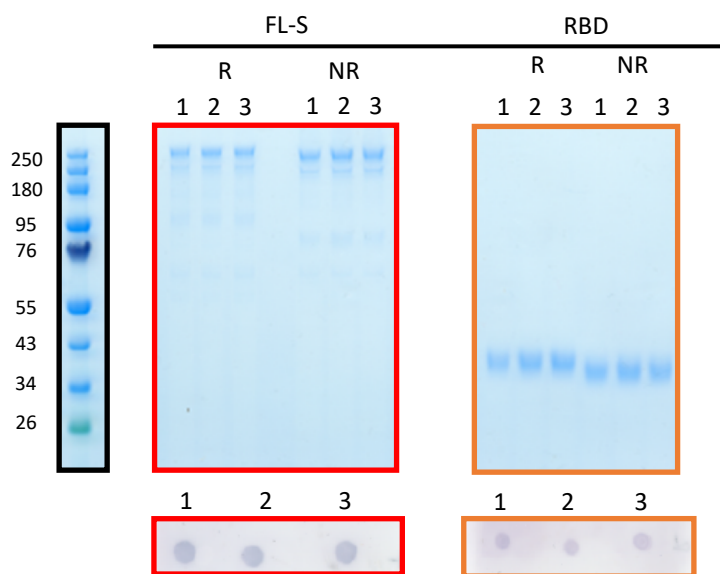
A**B****C**

Figure 1. A) Size exclusion chromatograms post-purification: 1. FL-NP; 2. FL-S; 3. CR3022; 4. RBD; and 5. ACE2. All proteins were run individually with chromatograms overlaid. Asterisk indicates the fraction run on SDS-PAGE. **B)** Non-reducing (NR) or reducing (R) Coomassie blue-stained SDS-PAGE protein gels of 1 µg of protein from the asterisk indicated fractions. **C)** Freeze-thaw stability of FL-S and RBD. Reducing and non-reducing SDS-PAGE protein gel of 1 µg FL-S (red panel) and RBD (orange panel) after 1, 2 and 3 freeze-thaw cycles. Below each gel a dot-blot is shown, using the CR3022 human mAb on 1 µg FL-S and RBD after 1, 2 and 3 freeze-thaw cycles.

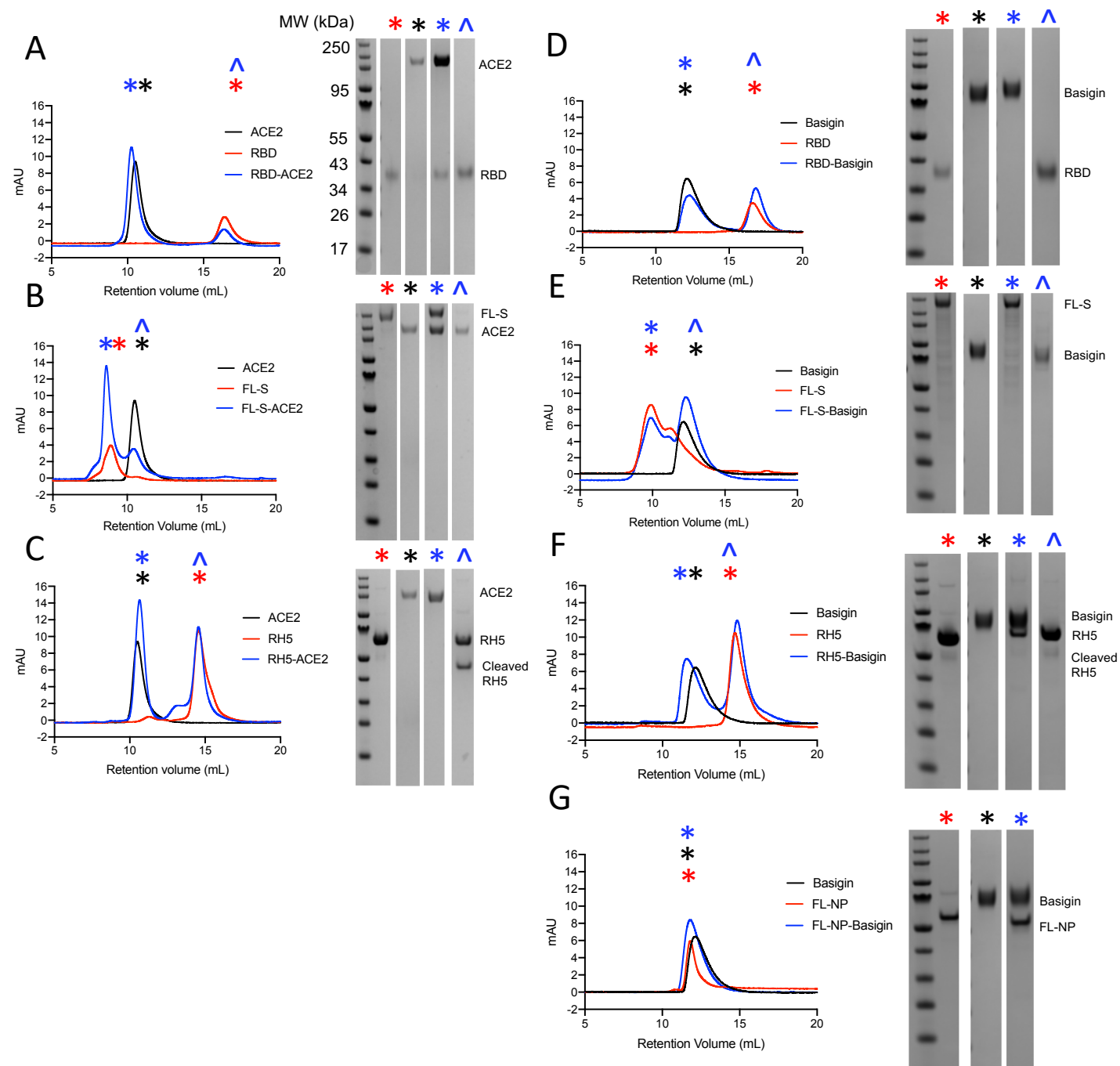


Figure 2. Size exclusion chromatograms (left) and accompanying SDS-PAGE gels (right) assessing complex formation between RH5/RBD/FL-S/RBD and ACE2/Basigin. Symbol on chromatogram indicates which gel corresponds to that peak. Full-length RH5 (~60 kDa) undergoes cleavage at room temperature to yield an ~43 kDa band. **A)** RBD-ACE2; **B)** FL-S-ACE2; **C)** RH5-ACE2; **D)** RBD-Basigin; **E)** FL-S-Basigin; **F)** RH5-Basigin; and **G)** FL-NP-Basigin.

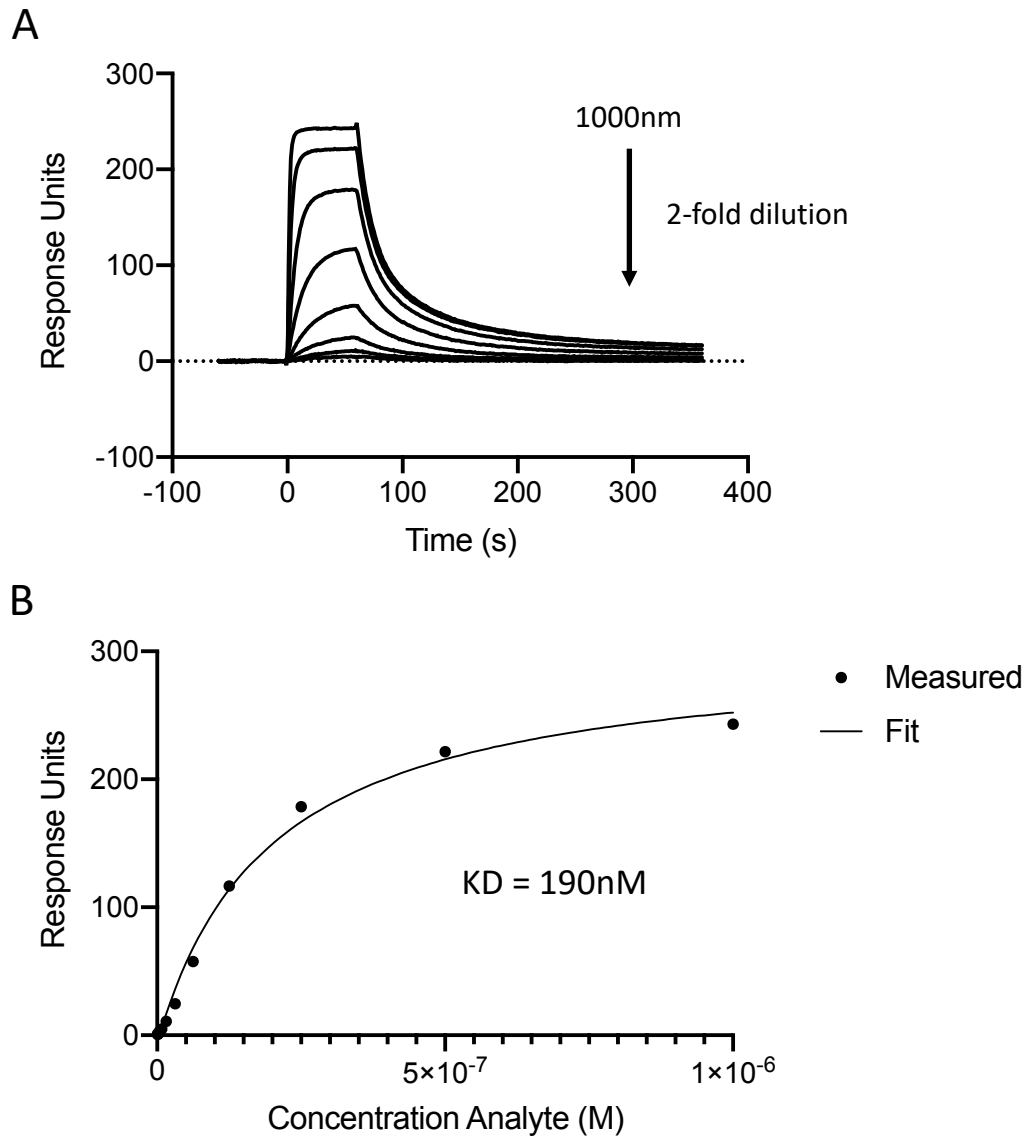


Figure 3. Steady state affinity of CR3022 mAb binding to RBD as assessed using SPR. **A)** Sensorgram of 8-step dilution curve beginning at 1 μ M. **B)** Calculation of steady-state affinity.

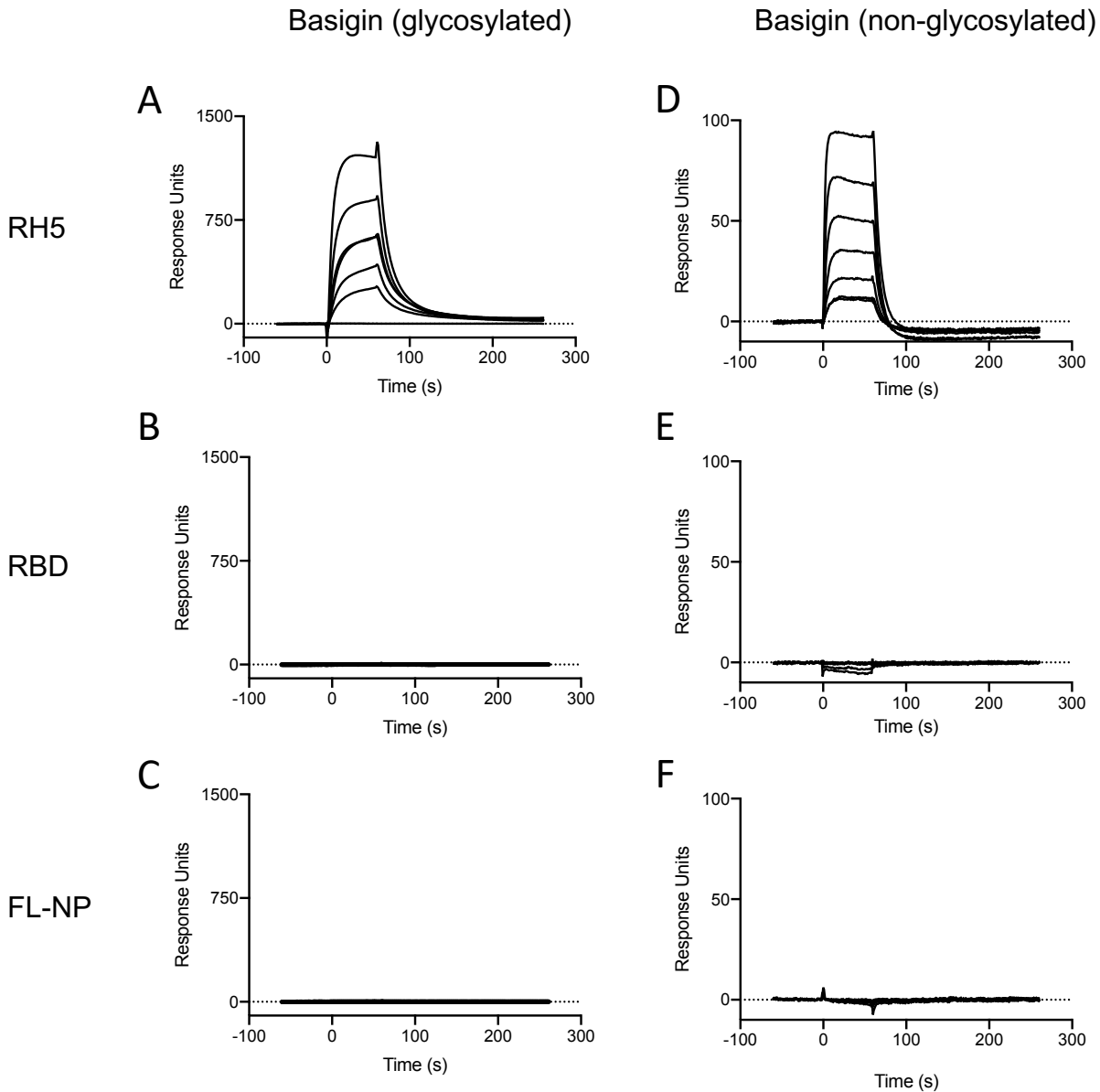


Figure 4. SPR analysis of protein binding interactions. Sensorgrams show binding of each protein to either glycosylated or non-glycosylated basigin (coupled to the chip). Protein binding was assessed along 5-step two-fold dilution curves starting at 2 μ M. **A)** Glycosylated basigin binding to RH5; **B)** Glycosylated basigin binding to RBD; **C)** Glycosylated basigin binding to FL-NP; **D)** Non-glycosylated basigin binding to RH5; **E)** Non-glycosylated basigin binding to RBD; **F)** Non-glycosylated basigin binding to FL-NP.

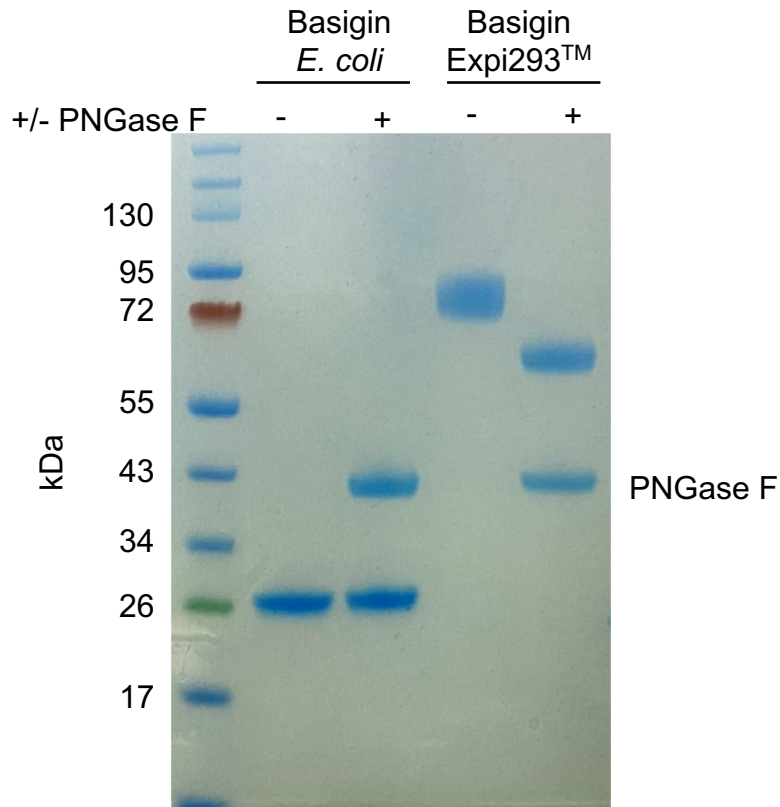


Figure S1. PNGase F digest of *E. coli*-expressed (non-glycosylated) and Expi293TM-expressed (glycosylated) basigin. The lower molecular weight of glycosylated basigin after PNGase F treatment is consistent with the loss of glycans. The heavier molecular weight of glycosylated basigin treated with PNGase F compared to non-glycosylated basigin can be attributed to the presence of the rat CD4 domains 3+4 (CD4d3+4) solubility tag (33 kDa).

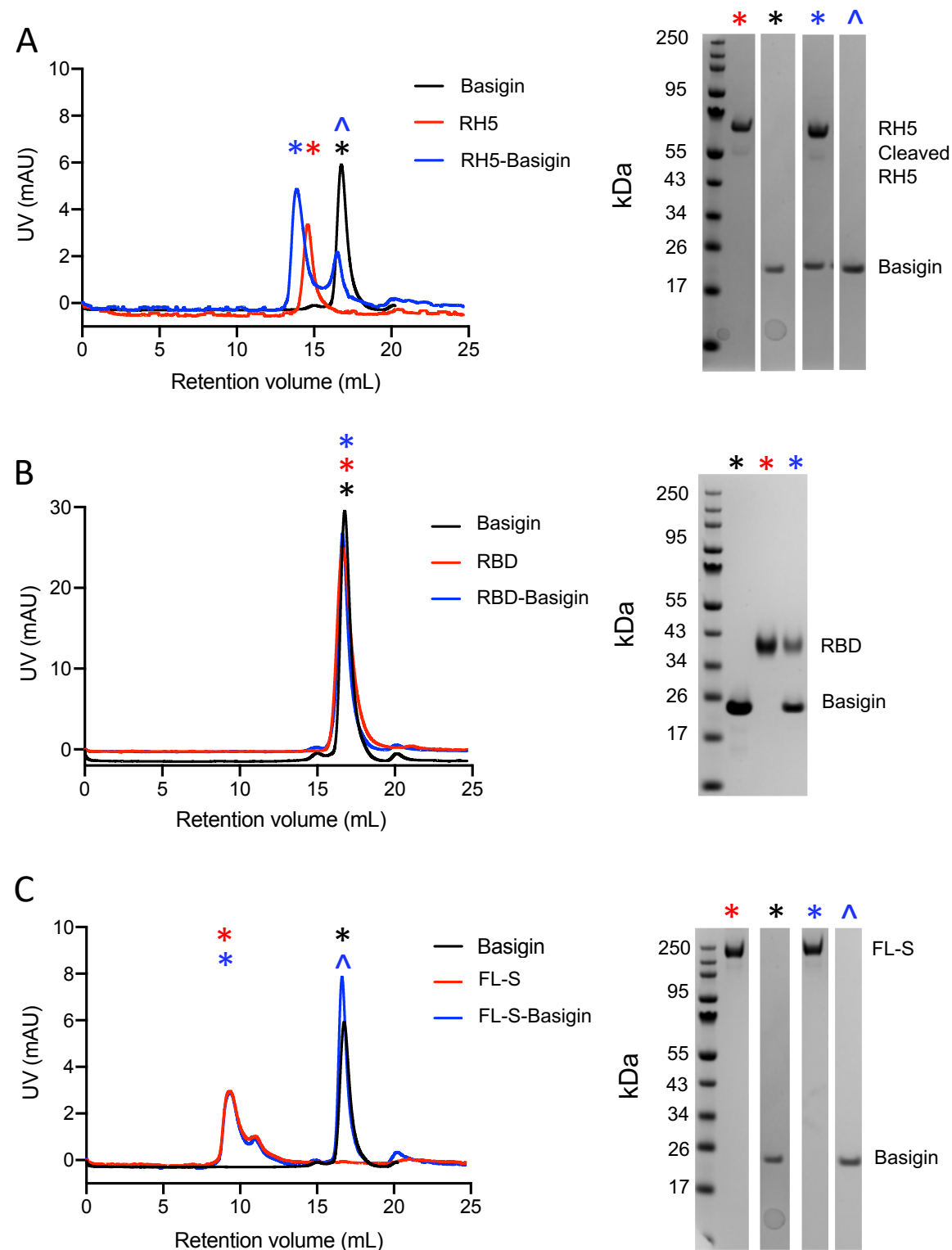


Figure S2. Size exclusion chromatograms (left) and accompanying SDS-PAGE gels (right) of non-glycosylated basigin binding to RH5/RBD/FL-S. **A)** RH5-Basigin; **B)** RBD-Basigin; **C)** FL-S-Basigin.